

• 临床研究 •

多模态影像学对乳腺导管原位癌病变范围评估性能的比较

瞿颖, 黄越, 李明卉, 孙畅, 王水*

南京医科大学第一附属医院乳腺外科, 江苏 南京 210029

[摘要] 目的: 比较乳腺X线摄影(mammography, MG)、超声(ultrasonography, US)和磁共振成像(magnetic resonance imaging, MRI)3种常规影像学检查在评估乳腺导管原位癌(ductal carcinoma *in situ*, DCIS)或DCIS伴微浸润(DCIS with microinvasion, DCIS-MI)病灶大小方面的效能, 探讨其辅助临床管理保乳患者的潜在价值。方法: 回顾性收集南京医科大学第一附属医院病理证实的DCIS/DCIS-MI患者的病例资料, 将3种影像学检查评估的病灶大小与“金标准”病理学大小比较, 采用McNemar检验和Bland-Altman法对不同成像方式进行准确性、一致性的评价。采用单因素与多因素分析明确影响评估准确性的临床病理特征, 并进行亚组分析。最后, 探索分析导致影像学检查结果为假阴性的影响因素。结果: 共入选263例DCIS/DCIS-MI患者。测量均值偏差方面, MRI多高估(+3.5 mm)病灶, 而MG(-2.5 mm)和US(-1.4 mm)低估。一致性分析提示MRI与病理结果相关性最强($r=0.853$), 95%一致性界限(95% limits of agreement, 95% LOA)范围最窄(-1.73~2.44 cm), 优于MG($r=0.561$)及US($r=0.614$)。McNemar准确性分析提示MRI准确性高于US和MG($P < 0.05$), 而二者联合使用后准确性与MRI相当($P=0.921$)。Logistic回归分析显示, 确诊时年龄 >60 岁(OR=0.322)、肿瘤直径16~40 mm(OR=3.019)和 ≥ 41 mm(OR=6.146)显著影响MG评估准确性($P < 0.05$)。肿瘤直径16~40 mm(OR=2.270)和 ≥ 41 mm(OR=4.237)及导管扩张征(OR=1.728)显著增加US评估误差风险($P < 0.05$)。中重度乳腺背景实质强化(OR=2.139)和非肿块样强化灶(OR=2.655)显著增加MRI评估误差风险($P < 0.05$)。亚组分析提示, 肿瘤直径 ≤ 15 mm, 3种影像学检查评估效能相近; 直径16~40 mm, 宜选择超声; 直径 ≥ 41 mm, 宜选择MRI。此外, HER2表达状态(OR=0.100)及Ki67表达水平(OR=0.297)是影响MG检出病灶的独立预测因子($P < 0.05$)。结论: 术前MRI检查有助于指导DCIS/DCIS-MI患者实现精准保乳, 尤其病灶直径 ≥ 41 mm时。在基层医院的临床诊疗工作中, 可进行超声联合乳腺X线检查。对于HER2和Ki67低表达的患者, 术前乳腺X线评估时应注意假阴性可能。

[关键词] 乳腺导管原位癌; 肿瘤大小; 乳腺X线摄影; 超声; 磁共振成像**[中图分类号]** R737.9**[文献标志码]** A**[文章编号]** 1007-4368(2025)06-798-12

doi: 10.7655/NYDXBNSN250208

Comparative performance of multimodal imaging for the assessment of lesion extent of breast ductal carcinoma *in situ*

QU Ying, HUANG Yue, LI Minghui, SUN Chang, WANG Shui*

Department of Breast Surgery, the First Affiliated Hospital of Nanjing Medical University, Nanjing 210029, China

[Abstract] **Objective:** To compare the efficacy of three conventional imaging tests, mammography (MG), ultrasonography (US), and magnetic resonance imaging (MRI), in assessing the lesion size of ductal carcinoma *in situ* (DCIS) or DCIS with microinvasion (DCIS-MI), and explore their potential value in guiding breast-conserving surgery. **Methods:** We retrospectively collected case files of patients with pathologically confirmed DCIS/DCIS-MI in our hospital, and compared the lesion sizes assessed by the three imaging modalities with the “gold standard” pathological size, and evaluated the accuracy and consistency of the different imaging modalities by using McNemar’s test and Bland-Altman’s method. Univariate and multivariate analyses were used to identify the clinicopathologic features that influenced the accuracy of the assessment, followed by subgroup analyses. Finally, the influencing factors leading to false-negative -imaging results were explored and analyzed. **Results:** A total of 263 patients with DCIS/DCIS-MI were enrolled in this study. Regarding the measurement mean deviation, MRI mostly overestimated (+3.5 mm) lesions, while MG (-2.5 mm) and US (-1.4 mm) underestimated them. Consistency analysis suggested that MRI had the strongest correlation with pathological findings ($r=0.853$) and

[基金项目] 国家自然科学基金(82172683)

*通信作者(Corresponding author), E-mail: shwang@njmu.edu.cn (ORCID: 0000-0003-3480-7585)

the narrowest range of 95% limits of agreement (95% LOA) (-1.73~2.44 cm), which was superior to MG ($r=0.561$) and US ($r=0.614$). McNemar test indicated MRI's superiority over US/MG ($P < 0.05$), while combined US+MG achieved comparable accuracy to MRI ($P=0.921$). Logistic regression analysis showed that age >60 years at diagnosis (OR=0.322), tumor diameter 16-40 mm (OR=3.019), and ≥ 41 mm (OR=6.146) significantly affected the accuracy of MG assessment (all $P < 0.05$). Tumor diameters of 16-40 mm (OR=2.270) and ≥ 41 mm (OR=4.237) and ductal dilatation sign (OR=1.728) significantly increased the risk of US assessment error (all $P < 0.05$). Moderate-to-severe breast background parenchymal enhancement (OR=2.139) and non-mass-like foci of enhancement (OR=2.655) significantly increased the risk of MRI assessment error (all $P < 0.05$). Subgroup analyses suggested comparable performance for lesions ≤ 15 mm, US preference for 16-40 mm lesions, and MRI advantage for ≥ 41 mm lesions. In addition, the HER2 expression status (OR=0.100) and the Ki67 expression level (OR=0.297) were independent predictors for MG detection failure (all $P < 0.05$).

Conclusion: Preoperative MRI is beneficial for guiding precise breast-conserving surgery in DCIS/DCIS-MI patients, particularly for lesions ≥ 41 mm. In clinical practice at primary hospitals, the combined use of US and MG can be promoted. For patients with low HER2 and Ki67 expression, the possibility of false-negative results should be considered during preoperative MG evaluation.

[Key words] ductal carcinoma in situ; tumor size; mammography; ultrasonography; magnetic resonance imaging

[J Nanjing Med Univ, 2025, 45(06): 798-809]

乳腺癌是全球女性最常见的癌症类型^[1]。随着女性患者愈发重视术后生存质量,且多项临床研究证实保乳手术联合放疗的安全性^[2-3],保乳率整体呈上升趋势。对于有保乳意愿的乳腺癌患者,术前检查低估肿瘤范围可能会增加二次手术率和局部复发风险,高估则可能导致手术切除范围过大,影响美容效果,故进行准确的临床评估至关重要。

目前,常规用于临床评估乳腺癌的影像学检查有乳腺X线摄影(mammography, MG)、超声(ultrasonography, US)和磁共振成像(magnetic resonance imaging, MRI)。MG是乳腺癌早期筛查的首选方法,对微小钙化尤为敏感^[4],但其灵敏度欠佳^[5]。US具有操作简单、无辐射及敏感性不受腺体密度影响等优势,但结果易受医生主观性影响。MRI可提供三维成像,评估肿瘤血供,还通过建立多参数影像组学模型为实际临床工作中乳腺癌患者表皮生长因子受体-2(human epidermal growth factor receptor-2, HER2)表达状态判读提供无创性的辅助工具;然而因其特异性较低和成本较高,通常仅用于高危女性的筛查诊断^[6-8]。上述检查各有特点,彼此能否互为补充,提高病灶的检出率及准确性尚不明确。

导管原位癌(ductal carcinoma *in situ*, DCIS)及伴微浸润(DCIS with microinvasion, DCIS-MI)因其沿导管生长、较少破坏正常腺体而不易形成占位性病变的生物学特性,导致其临床评估难度更高,接受保乳的患者二次手术率远高于其他病理类型^[9]。因此,术前需对此类拟保乳患者的病灶范围进行精准评估。基于此,本研究旨在系统比较MG、US和MRI

对于DCIS/DCIS-MI病变范围的评估效能,优化影像学评估策略,从而安全有效地提高DCIS/DCIS-MI患者的保乳率。

1 对象和方法

1.1 对象

本研究为回顾性分析,选取2020年1月—2024年12月于南京医科大学第一附属医院经术后常规病理证实为DCIS或DCIS-MI的患者,并于术前1个月内于本院接受MG、US及MRI检查,且影像图像和临床资料完整。本研究将DCIS-MI定义为具有1个或多个 ≤ 1.0 mm的浸润性灶的DCIS。主要排除标准:①年龄 <18 岁的女性患者,所有男性患者;②术前行抗肿瘤治疗,如新辅助化疗、内分泌治疗、靶向治疗或乳房及邻近脏器放射治疗;③外院肿块活检术后;④晚期乳腺癌或乳腺癌复发;⑤合并除乳腺癌以外的其他恶性肿瘤;⑥临床病理或影像资料不完整。本研究经南京医科大学第一附属医院伦理委员会审查批准(伦理号:2021-SR-185),符合《赫尔辛基宣言》伦理准则并豁免患者知情同意。

1.2 方法

1.2.1 一般资料

收集整理以下数据,包括①临床基本情况:确诊时年龄、体重指数(body mass index, BMI)、月经状态、乳腺癌家族史、原发灶手术史、腋窝手术史;②病理资料:腋窝淋巴结状态、肿瘤大小、病理学类型、组织学分级、雌激素受体(estrogen receptor, ER)、孕激素受体(progesterone receptor, PR)、HER2、Ki67、

P63和有无粉刺样坏死等;③影像学资料:MG显示腺体密度、病灶大小、病灶类型(假阴性、钙化、肿块、结构扭曲或局灶性不对称影)、钙化形态及分布;US显示病灶大小、病灶类型(假阴性、低回声区、导管扩张、肿块伴或不伴微钙化、结构扭曲、点状强回声)、肿块的形状、边缘、内部回声、后方回声及纵横比;MRI显示背景实质强化程度、病灶强化类型、病灶大小、TIC曲线等。

本研究中DCIS影像学检查结果阴性的标准为影像学上未见肿块、钙化、异常密度影、结构扭曲变形或其他可疑病变,经过2名具有5年以上乳腺影像诊断经验的放射科医生共同协商判定为BI-RADS 3级及以下类别,反之考虑为阳性病灶。

1.2.2 影像学设备与使用

MG使用德国Siemens MAMMOMAT Revelation乳腺机或美国GE Senographe Pristina数字化乳腺机完成头尾位和内外侧斜位的拍摄。US检查使用MyLab Twice、Philips、Mindray或Siemens彩色多普勒超声诊断仪,对患者双侧乳房4个象限、乳头乳晕区以及双侧腋窝反复扫查。MRI采用3.0 T(Trio Tim, Siemens公司,德国)和1.5 T(Aera, Siemens公司,德国)磁共振扫描仪和8通道乳腺线圈采集图像。所有患者均行乳腺MRI平扫及多期动态增强扫描。扫描序列包括:①快速反转恢复压脂序列横轴面T2WI;②横轴面弥散加权成像及其衍生表现观弥散系数图;③横轴面T1WI多期动态对比增强MRI。

由于本研究主要关注病灶大小这一形态学指标,而非功能性参数,且影像学检查设备的型号和制造商对病灶大小的测量结果影响较小,因此在研究设计阶段并未将使用不同型号影像设备的患者排除在外。

1.3 统计学方法

本研究使用的统计学软件为SPSS (version 27.0)及GraphPad Prism (version 9.5.0)。连续型变量用均数±标准差($\bar{x} \pm s$)表示;分类变量以例数(百分比)表示,组间差异使用卡方检验或Fisher精确概率法分析。McNemar检验用于比较MG、US和MRI对病灶评估的准确性。Pearson相关系数用于评估3种影像学评估的病灶范围与手术标本的组织病理学大小的线性相关性。使用Bland-Altman图评估影像学大小与病理学大小的一致性。将 $P < 0.05$ 的变量进一步纳入多因素Logistic回归分析,筛选成像大小与病理学大小之间一致性和影像学检查结果假阴性的影响因素。所有统计检验均为双

尾检验, $P < 0.05$ 为差异有统计学意义。

2 结果

2.1 临床病理特征

共纳入2020年1月—2024年12月于本院就诊的263例DCIS/DCIS-MI患者,其中,8例为双侧乳腺癌,4例为同侧乳房同时存在2个病灶,共计275个病灶。患者平均年龄为51岁(范围23~86岁)。临床病理特征详见表1。

2.2 影像学特征

DCIS/DCIS-MI患者中,29例(10.5%)MG呈阴性表现,13例(4.7%)US未见明显异常,MRI检查无漏诊。患者的影像学特征详见表2。

2.3 比较不同影像学检查评估导管原位癌病变范围的效能

排除前述假阴性病例,MG和US的术前成像低估了实际大小,MRI多倾向于高估。以 ± 5 mm作为术前影像学 and 病理学大小一致的阈值,结果显示,对于DCIS/DCIS-MI病灶,MRI的影像学 with 病理学一致率最高(表3)。相关性分析显示,在DCIS/DCIS-MI中,MG、US、MRI以及MG联合US检查的相关系数分别为0.561、0.614、0.853和0.632($P < 0.001$)。此外,MRI的95%一致性界限(95% limits of agreement, 95% LOA)宽度最窄(-1.73~2.44 cm),即相比MG和US,MRI与实际组织病理学评估的病变大小一致性更佳(图1)。3种影像学检查方法准确性的比较结果显示,MRI术前评估的准确性显著高于MG与US(P 均 < 0.05)。考虑到基层医疗机构中MRI的普及率较低,为了明确临床工作中联合应用MG和US是否可达到MRI的效能,进一步将联合检查的准确性与MRI比较。结果显示,在DCIS/DCIS-MI患者中联合使用MG和US的准确性与MRI相当($\chi^2 = 0.039, P = 0.921$,表4)。

2.4 影响影像学检查评估病变范围准确性的因素

为进一步明确影响术前影像学评估病灶范围准确性的临床、病理因素,参照前述以 ± 5 mm为标准,将入选DCIS/DCIS-MI患者分为评估准确组和误差组。单因素和多因素Logistic分析显示,确诊时年龄和肿瘤直径显著影响MG对导管原位癌术前评估的准确性。 > 60 岁的老年患者($OR = 0.322, P = 0.039$)病变评估发生误差的可能性更小;与直径 ≤ 15 mm的病灶相比,MG对直径16~40 mm($OR = 3.019, P < 0.001$)和 ≥ 41 mm($OR = 6.146, P < 0.001$)的病灶评估发生误差的风险更高(表5)。

表1 入组患者的临床、病理特征
Table 1 Clinical and pathological characteristics of enrolled patients

| Characteristic | Value[n(%)] | Characteristic | Value[n(%)] |
|--------------------------|-------------|---------------------------------|-------------|
| Age | | Comedo necrosis | |
| ≤39 years | 36(13.7) | Present | 155(56.4) |
| 40~60 years | 186(70.7) | Absent | 120(43.6) |
| >60 years | 41(15.6) | ER | |
| Menopausal status | | Negative | 75(27.3) |
| Yes | 124(47.1) | Positive | 200(72.7) |
| No | 139(52.9) | PR | |
| BMI classification | | Negative | 102(37.1) |
| Underweight | 17(6.5) | Positive | 173(62.9) |
| Normal | 185(70.3) | HER2 | |
| Obese | 56(21.3) | 0 | 50(18.2) |
| Overweight | 5(1.9) | 1+ | 75(27.3) |
| Gland density | | 2+ | 62(22.5) |
| Fatty | 8(3.0) | 3+ | 88(32.0) |
| Scattered fibroglandular | 39(14.4) | Ki67 | |
| Heterogeneously dense | 191(70.5) | Low | 119(43.3) |
| Dense | 33(12.2) | High | 156(56.7) |
| Tumor diameter | | P63 | |
| ≤15 mm | 116(42.2) | Negative | 75(27.3) |
| 16~40 mm | 119(43.3) | Positive | 200(72.7) |
| ≥41 mm | 40(14.5) | Breast surgery | |
| Pathological type | | Breast-conserving surgery | 81(29.9) |
| DCIS | 170(61.8) | Mastectomy | 190(70.1) |
| DCIS-MI | 105(38.2) | Axillary lymph node status | |
| Histological grade | | Negative | 268(98.9) |
| Grade I | 25(9.1) | Positive | 3(1.1) |
| Grade II | 130(47.3) | Family history of breast cancer | |
| Grade III | 120(43.6) | Yes | 11(4.2) |
| | | No | 252(95.8) |

在超声检查中,肿瘤直径以及有无导管扩张均为影响评估准确性的独立预测因子。与直径≤15 mm的病灶相比,直径16~40 mm(OR=2.270, $P=0.003$)、直径≥41mm(OR=4.237, $P < 0.001$)以及存在导管扩张(OR=1.728, $P=0.042$)的导管原位癌US病灶评估发生误差可能性更大(表6)。背景实质强化程度和病灶强化类型显著影响MRI的评估准确性。中重度背景实质强化(OR=2.139, $P=0.007$)和呈非肿块样强化灶(non-mass enhancement, NME)(OR=2.655, $P < 0.001$)的患者术前MRI评估产生误差的可能性更大(表7)。同时上述3种影像学检查相关的预测模型均经 Hosmer - Lemeshow 检验 ($P=0.702$, $P=0.997$, $P=0.907$),模型拟合良好。

由上述分析可知,肿瘤直径是影响MG和US术

前预测导管原位癌病变范围准确性的一个重要因素,故参照 van Nuys 预后指数中的肿瘤直径评分标准进行亚组分析。据箱线图所示(图2),对于直径≤15 mm的DCIS/DCIS-MI病灶,3种影像学检查的评估效能相近。对于直径16~40 mm的病灶,US成像更具优势。对于病变广泛(直径≥41 mm)的病灶,MRI的精准成像和术前评估能力优于2种传统成像。

2.5 影响影像学检查结果假阴性发生的因素

最后对本研究中的MG假阴性病例进行分析,在DCIS/DCIS-MI患者中,HER2表达状态及Ki67表达水平是影响MG检出病灶的独立预测因子,即HER2(OR=0.100, $P=0.034$)及Ki67(OR=0.297, $P=0.026$)低表达的导管原位癌病灶更易在MG中被忽略(表8)。本研究中US仅有13例未检出,样本量较

表2 入组患者的影像学特征
Table 2 Imaging characteristics of enrolled patients

| Imaging feature | Value[n(%)] | Imaging feature | Value[n(%)] |
|--|-------------|------------------------------------|-------------|
| MG features | | Mass margin | |
| False negative | 29(10.5) | Smooth | 61(36.3) |
| Architectural distortion | 18(6.5) | Unsmooth | 107(63.7) |
| Focal asymmetry | 53(19.3) | Internal echo of mass | |
| Mass | 68(24.7) | Hypoechoic | 156(92.9) |
| Calcification | 107(38.9) | Complex cystic and solid | 12(7.1) |
| MG calcification morphology | | Posterior echo of mass | |
| Suspicious malignant | 104(37.8) | No change | 162(96.4) |
| None or typical benign | 171(62.2) | Attenuation | 6(3.6) |
| MG suspicious calcification distribution | | Mass aspect ratio | |
| Clustered | 51(47.7) | ≥1 | 11(6.5) |
| Linear/Segmental | 23(21.5) | <1 | 157(93.5) |
| Regional | 17(15.9) | MRI lesion enhancement type | |
| Diffuse/Scattered | 16(15.0) | Mass-like enhancement | 113(41.1) |
| US features | | Non-massenhancement | 162(58.9) |
| False negative | 13(4.7) | Background parenchymal enhancement | |
| Ductal ectasia | 31(11.3) | Minimal | 45(16.6) |
| Hypoechoic area | 46(16.7) | Mild | 146(53.9) |
| Structural disorganization | 12(4.4) | Moderate | 50(18.5) |
| Mass | 168(61.1) | Marked | 30(11.1) |
| Punctate echogenic foci | 5(1.8) | TIC curve | |
| Mass shape | | Inflow | 54(19.6) |
| Regular | 47(28.0) | Plateau | 168(61.1) |
| Irregular | 121(72.0) | Outflow | 53(19.3) |

表3 影像学检查与病理学肿瘤大小的对比及偏差分析
Table 3 Comparison and deviation analysis of tumor size on imaging and pathology

| Variable | MG (n=246) | US (n=262) | MRI (n=275) |
|------------------|---------------|---------------|----------------|
| Agreement[n(%)] | 95(38.6) | 125(47.7) | 156(56.7) |
| Over estimation | 59(24.0) | 69(26.3) | 90(32.7) |
| Under estimation | 92(37.4) | 68(26.0) | 29(10.5) |

小,故未进行分析。

3 讨论

目前癌症管理进入个体化与精准化的时代,乳腺癌患者的保乳率整体呈上升趋势。DCIS患者因其肿瘤生物学特性导致保乳后再手术率较高,因此,术前对病灶进行充分的影像学评估至关重要。本研究主要就3种常规影像学检查包括MG、US和MRI评估病变范围的能力进行比较,拟为DCIS保乳患者的临床诊疗提供一定指导意见。

首先,本研究入选患者的影像学表现中,MG的假阴性率最高(10.5%)。与本文数据类似,其他研究表明,MRI在诊断DCIS方面优于MG和US^[10-11]。在对本研究中的假阴性病例分析发现,HER2表达状态及Ki67表达水平是影响MG检出导管内癌病灶的独立预测因子。既往多项研究指出,DCIS的MG影像特征与免疫组织化学分子亚型具有相关性。超过80%的HER2过表达亚型表现为细小多形性、细线分支样及线样和段样分布的钙化^[12],而约有70% DCIS病例正是仅通过存在微钙化来诊断的^[13],故HER2高表达的病灶可能更不容易被忽略。此外,近期研究表明,基于多参数影像特征构建的影像组学模型评估浸润性乳腺癌HER-2表达状态有一定的临床价值。

本研究结果显示,MG和US多低估病灶大小,MRI则倾向高估。关于MG,钙化分布不均掩盖边缘^[14-15]。并且MG也存在一定的摄影盲区,如乳房边缘尤其是靠近腋窝位置。US低估原因可能是

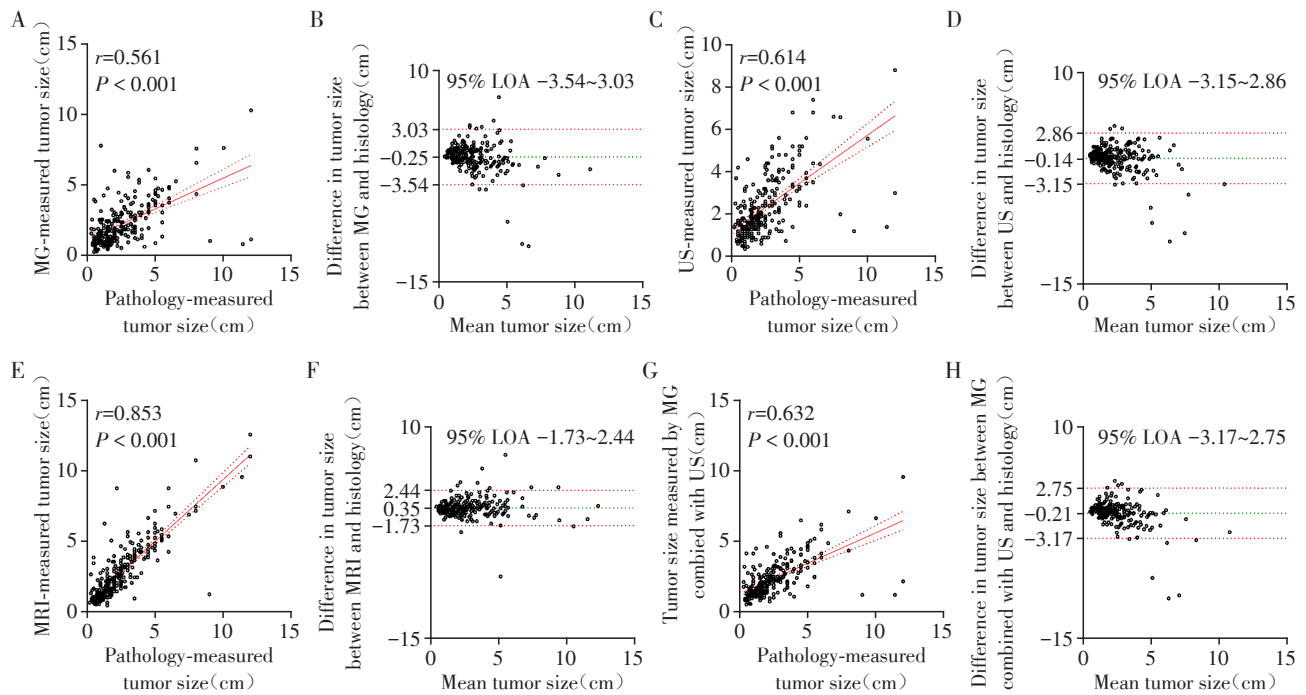


图1 3种影像学检查以及MG联合US评估的DCIS/DCIS-MI病变范围与病理学大小的相关性和一致性

Figure 1 Correlation and concordance between DCIS/DCIS-MI lesion extent and histopathologic size as assessed by the three imaging tests and MG combined US

表4 3种影像学检查术前评估病灶范围准确性的比较

Table 4 Comparison of the accuracy of three imaging tests for preoperative assessment of lesion extent

| Examination A vs. B | n_{01} | n_{10} | χ^2 | P |
|---------------------|----------|----------|----------|--------|
| MG vs. US | 23 | 41 | 5.063 | 0.033 |
| MG vs. MRI | 32 | 68 | 12.960 | <0.001 |
| US vs. MRI | 37 | 57 | 4.255 | 0.049 |
| (MG+US) vs. MRI | 50 | 52 | 0.039 | 0.921 |

The difference between imaging and pathological lesion size ≤ 5 mm was assigned a value of 0 (accurate), and >5 mm was assigned a value of 1 (inaccurate). n_{01} refers to the number of patients where method A was accurate and method B was inaccurate; n_{10} refers to the number of patients where method A was inaccurate and method B was accurate.

广泛导管内癌致超声成像边缘不明确; 肿瘤体积较大, 图像呈现超出了换能器水平; 或受探头宽度范围和压力调节的限制。与前述两种影像学检查不同, 本研究中MRI“高估”了病灶大小, 其原因可能是中重度背景实质增强, 如肿瘤内导管内成分或纤维组织成分占比更高^[10, 16]。此外, 由于标本塌陷和甲醛固定后收缩, 组织病理学可能本身就低估了病灶大小^[17], 故MRI或许代表了实际的病灶范围。

本研究中, MRI的准确性和一致性也强于其他两种传统影像学检查。在DCIS/DCIS-MI患者中,

MG联合US检查的准确性与MRI相当, 提示在当前基层医院中MRI尚未普及并不一定增加保乳术后的二次手术风险, 但是由于联合检查的一致性较低, 故保乳外观和患者满意度可能受到一定程度影响。多项研究报道了MRI术前评估的潜在价值^[18-20], 但也有研究指出^[21], MG在评估DCIS病变大小方面与MRI无明显差异。然而, 这些研究均是回顾性的, 用于评定影像学大小与病理学大小一致性的标准也各不相同, 故可能产生上述差异。

对成像大小与病理大小一致性的影响因素分析提示, 肿瘤直径是影响成像大小准确性的重要因素。故将患者分组进行亚组分析, 结果表明对于直径 ≥ 41 mm的导管原位癌, MRI成像范围更准确。因此, 如果计划对病灶广泛的患者行保乳手术, 则可以通过MRI高精度评估局部疾病范围。即便对于多中心性的患者, 也可通过术前活检和重点评估可疑病变来规避由此引起的不必要全乳切除。

本研究不可避免存在少许不足。首先, 本研究为回顾性研究, 样本量相对较小, 并且数据来自单一机构, 不可避免样本数据偏倚问题, 今后仍需进一步开展大规模、前瞻性、多中心研究提高结果可信度。其次, 本研究由影像科医生读取影像特征并撰写报告, 可能存在一定的主观偏差, 未来应联合应用人

表5 影响MG术前评估DCIS/DCIS-MI范围准确性的单因素和多因素分析

Table 5 Univariate and multivariate analyses affecting the accuracy of DCIS/DCIS-MI ranges in preoperative MG assessment

| Characteristic | Accurate group (n=95) | Inaccurate group (n=151) | χ^2 | P | Multivariate analysis | | |
|--------------------------|--------------------------|-----------------------------|----------|--------|-----------------------|--------------|--------|
| | | | | | OR | 95%CI | P |
| Age | | | 12.003 | 0.002 | | | |
| ≤39 years | 8(8.4) | 25(16.6) | | | | | Ref. |
| 40–60 years | 62(65.3) | 110(72.8) | | | 0.724 | 0.293–1.789 | 0.484 |
| >60 years | 25(26.3) | 16(10.6) | | | 0.322 | 0.109–0.946 | 0.039 |
| Menopausal status | | | 1.216 | 0.270 | | | |
| Yes | 49(51.6) | 67(44.4) | | | | | |
| No | 46(48.4) | 84(55.6) | | | | | |
| BMI classification | | | 1.366 | 0.243 | | | |
| ≤25 kg/m ² | 80(84.2) | 118(78.1) | | | | | |
| >25 kg/m ² | 15(15.8) | 33(21.9) | | | | | |
| Gland density | | | – | 0.068 | | | |
| Fatty | 5(5.3) | 3(2.0) | | | | | |
| Scattered fibroglandular | 15(15.8) | 21(13.9) | | | | | |
| Heterogeneously dense | 58(61.1) | 113(74.8) | | | | | |
| Dense | 17(17.9) | 14(9.3) | | | | | |
| Tumor diameter | | | 28.322 | <0.001 | | | |
| ≤15 mm | 56(58.9) | 40(26.5) | | | | | Ref. |
| 16–40 mm | 33(34.7) | 78(51.7) | | | 3.019 | 1.659–5.496 | <0.001 |
| ≥41 mm | 6(6.3) | 33(21.9) | | | 6.146 | 2.282–16.549 | <0.001 |
| Pathological type | | | 2.140 | 0.143 | | | |
| DCIS | 63(66.3) | 86(57.0) | | | | | |
| DCIS-MI | 32(33.7) | 65(43.0) | | | | | |
| Histological grade | | | 5.704 | 0.058 | | | |
| Grade I | 13(13.7) | 8(5.3) | | | | | |
| Grade II | 44(46.3) | 70(46.4) | | | | | |
| Grade III | 38(40.0) | 73(48.3) | | | | | |
| Comedo necrosis | | | 5.735 | 0.017 | | | |
| Present | 48(50.5) | 53(35.1) | | | | | Ref. |
| Absent | 47(49.5) | 98(64.9) | | | 1.158 | 0.615–2.179 | 0.650 |
| ER | | | 2.079 | 0.100 | | | |
| Negative | 21(22.1) | 48(31.8) | | | | | |
| Positive | 74(77.9) | 103(68.2) | | | | | |
| PR | | | 2.041 | 0.153 | | | |
| Negative | 31(32.6) | 63(41.7) | | | | | |
| Positive | 64(67.4) | 88(58.3) | | | | | |
| HER2 | | | 5.909 | 0.052 | | | |
| 0–1+ | 48(50.5) | 53(35.1) | | | | | |
| 2+ | 20(21.1) | 38(25.2) | | | | | |
| 3+ | 27(28.4) | 60(39.7) | | | | | |
| Ki67 | | | 4.528 | 0.033 | | | |
| Low | 45(47.4) | 51(33.8) | | | | | Ref. |
| High | 50(52.6) | 100(66.2) | | | 1.232 | 0.653–2.327 | 0.520 |
| P63 | | | 0.090 | 0.764 | | | |
| Negative | 26(27.4) | 44(29.1) | | | | | |
| Positive | 69(72.6) | 107(70.9) | | | | | |
| MG features | | | 2.953 | 0.399 | | | |
| Calcification | 39(41.1) | 68(45.0) | | | | | |
| Architectural distortion | 6(6.3) | 12(7.9) | | | | | |
| Focal asymmetry | 18(18.9) | 35(23.2) | | | | | |
| Mass | 32(33.7) | 36(23.8) | | | | | |

表6 影响US术前评估DCIS/DCIS-MI范围准确性的单因素和多因素分析

Table 6 Univariate and multivariate analyses affecting the accuracy of DCIS/DCIS-MI ranges in preoperative US assessment

| Characteristic | Accurate group (n=125) | Inaccurate group (n=137) | χ^2 | P | Multivariate analysis | | |
|--------------------------|---------------------------|-----------------------------|----------|--------|-----------------------|-------------|--------|
| | | | | | OR | 95%CI | P |
| Age | | | 1.740 | 0.419 | | | |
| ≤39 years | 13(10.4) | 20(14.6) | | | | | |
| 40-60 years | 88(70.4) | 97(70.8) | | | | | |
| >60 years | 24(19.2) | 20(14.6) | | | | | |
| Menopausal status | | | 0.002 | 0.968 | | | |
| Yes | 59(47.2) | 65(47.4) | | | | | |
| No | 66(52.8) | 72(52.6) | | | | | |
| BMI classification | | | 0.433 | 0.511 | | | |
| ≤25 kg/m ² | 100(80.0) | 105(76.6) | | | | | |
| >25 kg/m ² | 25(20.0) | 32(23.4) | | | | | |
| Gland density | | | - | 0.516 | | | |
| Fatty | 5(4.0) | 3(2.2) | | | | | |
| Scattered fibroglandular | 20(16.0) | 15(10.9) | | | | | |
| Heterogeneously dense | 85(68.0) | 100(73.0) | | | | | |
| Dense | 15(12.0) | 19(13.9) | | | | | |
| Tumor diameter | | | 16.885 | <0.001 | | | |
| ≤15 mm | 67(53.6) | 42(30.7) | | | | | Ref. |
| 16-40 mm | 48(38.4) | 67(48.9) | | | 2.270 | 1.322-3.896 | 0.003 |
| ≥41 mm | 10(8.0) | 28(20.4) | | | 4.237 | 1.856-9.669 | <0.001 |
| Pathological type | | | 1.132 | 0.287 | | | |
| DCIS | 81(64.8) | 80(58.4) | | | | | |
| DCIS-MI | 44(35.2) | 57(41.6) | | | | | |
| Histological grade | | | 5.668 | 0.059 | | | |
| Grade I | 17(13.6) | 7(5.1) | | | | | |
| Grade II | 57(45.6) | 68(49.6) | | | | | |
| Grade III | 51(40.8) | 62(45.3) | | | | | |
| Comedo necrosis | | | 0.120 | 0.729 | | | |
| Present | 72(57.6) | 76(55.5) | | | | | |
| Absent | 53(42.4) | 61(44.5) | | | | | |
| ER | | | 1.840 | 0.175 | | | |
| Negative | 29(23.2) | 42(30.7) | | | | | |
| Positive | 96(76.8) | 95(69.3) | | | | | |
| PR | | | 0.004 | 0.950 | | | |
| Negative | 47(37.6) | 51(37.2) | | | | | |
| Positive | 78(62.4) | 86(62.8) | | | | | |
| HER2 | | | 0.171 | 0.918 | | | |
| 0-1+ | 53(42.4) | 61(44.5) | | | | | |
| 2+ | 29(23.2) | 32(23.4) | | | | | |
| 3+ | 43(34.4) | 44(32.1) | | | | | |
| Ki67 | | | 3.107 | 0.078 | | | |
| Low | 60(48.0) | 51(37.2) | | | | | |
| High | 65(52.0) | 86(62.8) | | | | | |
| P63 | | | 1.030 | 0.310 | | | |
| Negative | 39(31.2) | 35(25.5) | | | | | |
| Positive | 86(68.8) | 102(74.5) | | | | | |
| Ductal ectasia | | | 5.009 | 0.025 | | | |
| Absent | 87(69.6) | 77(56.2) | | | | | Ref. |
| Present | 38(30.4) | 60(43.8) | | | 1.728 | 1.020-2.929 | 0.042 |
| US features | | | 0.002 | 0.969 | | | |
| Mass-like | 80(64.0) | 88(64.2) | | | | | |
| Non-mass-like | 45(36.0) | 49(35.8) | | | | | |

表7 影响MRI术前评估DCIS/DCIS-MI范围准确性的单因素和多因素分析

Table 7 Univariate and multivariate analyses affecting the accuracy of DCIS/DCIS-MI Ranges in preoperative MRI assessment

| Characteristic | Accurate group (n=156) | Inaccurate group (n=119) | χ^2 | P | Multivariate analysis | | |
|------------------------------------|---------------------------|-----------------------------|----------|--------|-----------------------|-------------|--------|
| | | | | | OR | 95%CI | P |
| Age | | | 1.217 | 0.544 | | | |
| ≤39 years | 18(11.5) | 18(20.9) | | | | | |
| 40–60 years | 110(70.5) | 84(64.2) | | | | | |
| >60 years | 28(17.9) | 17(14.9) | | | | | |
| Menopausal status | | | 0.169 | 0.681 | | | |
| Yes | 76(48.7) | 55(52.2) | | | | | |
| No | 80(51.3) | 64(47.8) | | | | | |
| BMI classification | | | 1.415 | 0.234 | | | |
| ≤25 kg/m ² | 126(80.8) | 89(74.8) | | | | | |
| >25 kg/m ² | 30(19.2) | 30(25.2) | | | | | |
| Gland density | | | 0.187 | 0.665 | | | |
| Fatty | 5(3.2) | 3(2.5) | | | | | |
| Scattered fibroglandular | 23(14.7) | 16(13.4) | | | | | |
| Heterogeneously dense | 108(69.2) | 84(70.6) | | | | | |
| Dense | 20(12.8) | 16(13.4) | | | | | |
| Tumor diameter | | | 11.342 | 0.003 | | | |
| ≤15 mm | 79(50.6) | 37(31.1) | | | | | Ref. |
| 16–40 mm | 60(38.5) | 59(49.6) | | | 1.661 | 0.948–2.909 | 0.076 |
| ≥41 mm | 17(10.9) | 23(19.3) | | | 1.702 | 0.765–3.788 | 0.192 |
| Pathological type | | | 2.704 | 0.100 | | | |
| DCIS | 103(66.0) | 67(56.3) | | | | | |
| DCIS-MI | 53(34.0) | 52(43.7) | | | | | |
| Histological grade | | | 1.261 | 0.532 | | | |
| Grade I | 16(10.3) | 9(7.6) | | | | | |
| Grade II | 76(48.7) | 54(45.4) | | | | | |
| Grade III | 64(41.0) | 56(47.1) | | | | | |
| Comedo necrosis | | | 0.135 | 0.714 | | | |
| Present | 87(55.8) | 69(58.0) | | | | | |
| Absent | 69(44.2) | 50(42.0) | | | | | |
| ER | | | 0.939 | 0.333 | | | |
| Negative | 39(25.0) | 36(30.3) | | | | | |
| Positive | 117(75.0) | 83(69.7) | | | | | |
| PR | | | 0.520 | 0.471 | | | |
| Negative | 55(35.3) | 47(39.5) | | | | | |
| Positive | 101(64.7) | 72(60.5) | | | | | |
| HER2 | | | 3.610 | 0.164 | | | |
| 0–1+ | 76(48.7) | 45(37.8) | | | | | |
| 2+ | 34(21.8) | 28(23.5) | | | | | |
| 3+ | 46(29.5) | 46(38.7) | | | | | |
| Ki67 | | | 0.789 | 0.372 | | | |
| Low | 70(44.9) | 47(39.5) | | | | | |
| High | 86(55.1) | 72(60.5) | | | | | |
| P63 | | | 0.939 | 0.333 | | | |
| Negative | 39(25.0) | 36(30.2) | | | | | |
| Positive | 117(75.0) | 83(69.7) | | | | | |
| Background parenchymal enhancement | | | 7.057 | 0.008 | | | |
| Minimal and mild | 120(76.9) | 74(62.2) | | | | | Ref. |
| Moderate to marked | 36(23.1) | 45(37.8) | | | 2.139 | 1.226–3.733 | 0.007 |
| MRI lesion enhancement type | | | 17.475 | <0.001 | | | |
| Mass-like enhancement | 81(51.9) | 32(26.9) | | | | | Ref. |
| NME | 75(48.1) | 87(73.1) | | | 2.655 | 1.523–4.629 | <0.001 |

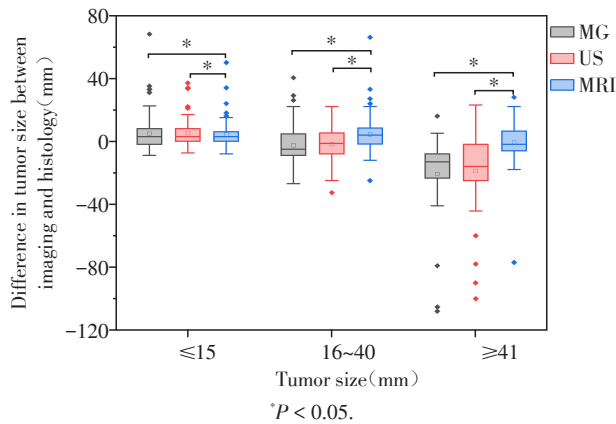


图2 不同直径的导管原位癌成像大小与病理学大小间的差值箱线图

Figure 2 Box line plot of the difference between imaging size and pathologic size for ductal carcinoma in situ of different diameters

工智能和放射组学等较为先进、敏感的技术。

本研究旨在提高术前影像学检查对病灶范围评估的准确性, 以在确保手术安全性的基础上, 进一步提升保乳手术的成功率, 并为临床决策提供重要依据。通过系统比较3种影像学检查在病灶范围评估中的效能, 本研究得出结论: 术前MRI成像在拟行保乳手术的DCIS/DCIS-MI患者的临床管理中具有重要价值, 建议保乳患者优先接受术前MRI检查。然而, 在基层医疗机构, 若缺乏MRI设备, 可采用MG联合US检查作为替代方案, 在一定程度上满足术前评估需求。

利益冲突声明:

全体作者均声明无利益冲突。

Conflict of Interests:

All authors declare no conflict of interests.

表8 影响DCIS/DCIS-MI病灶MG检查结果假阴性的单因素和多因素分析

Table 8 Univariate and multivariate analyses influencing false-negative MG findings in DCIS/DCIS-MI lesions

| Characteristic | Detected group (n=246) | Undetected group (n=29) | χ^2 | P | Multivariate analysis | | |
|--------------------------|---------------------------|----------------------------|----------|-------|-----------------------|-------------|-------|
| | | | | | OR | 95%CI | P |
| Age | | | - | 0.863 | | | |
| ≤39 years | 33(13.4) | 3(10.3) | | | | | |
| 40-60 years | 172(69.9) | 22(75.9) | | | | | |
| >60 years | 41(16.7) | 4(13.8) | | | | | |
| Menopausal status | | | 0.217 | 0.641 | | | |
| Yes | 116(47.2) | 15(51.7) | | | | | |
| No | 130(52.8) | 14(48.3) | | | | | |
| BMI classification | | | 1.614 | 0.204 | | | |
| ≤25 kg/m ² | 195(79.3) | 20(69.0) | | | | | |
| >25 kg/m ² | 51(20.7) | 9(31.0) | | | | | |
| Gland density | | | - | 0.774 | | | |
| Fatty | 8(3.3) | 0 | | | | | |
| Scattered fibroglandular | 36(14.6) | 3(10.3) | | | | | |
| Heterogeneously dense | 168(68.3) | 23(79.3) | | | | | |
| Dense | 34(13.8) | 3(10.3) | | | | | |
| Tumor diameter | | | 10.101 | 0.006 | | | |
| ≤15 mm | 96(39.0) | 20(69.0) | | | | | Ref. |
| 16-40 mm | 111(45.1) | 8(27.6) | | | 0.494 | 0.194-1.254 | 0.138 |
| ≥41 mm | 39(15.9) | 1(3.4) | | | 0.175 | 0.021-1.443 | 0.105 |
| Pathological type | | | 1.542 | 0.214 | | | |
| DCIS | 149(60.6) | 21(72.4) | | | | | |
| DCIS-MI | 97(39.4) | 8(27.6) | | | | | |
| Histological grade | | | 2.395 | 0.302 | | | |
| Grade I | 21(8.5) | 4(13.8) | | | | | |
| Grade II | 114(46.3) | 16(55.2) | | | | | |
| Grade III | 111(45.1) | 9(31.0) | | | | | |
| Comedo necrosis | | | 4.666 | 0.031 | | | |
| Present | 101(41.1) | 18(62.1) | | | | | Ref. |
| Absent | 145(58.9) | 11(37.9) | | | 1.598 | 0.611-4.176 | 0.339 |

(续表8)

| Characteristic | Detected group (n=246) | Undetected group (n=29) | χ^2 | P | Multivariate analysis | | |
|----------------|---------------------------|----------------------------|----------|--------|-----------------------|-------------|-------|
| | | | | | OR | 95%CI | P |
| ER | | | 0.708 | 0.400 | | | |
| Negative | 69(28.0) | 6(20.7) | | | | | |
| Positive | 177(72.0) | 23(79.3) | | | | | |
| PR | | | 1.255 | 0.263 | | | |
| Negative | 94(38.2) | 8(27.6) | | | | | |
| Positive | 152(61.8) | 21(72.4) | | | | | |
| HER2 | | | 19.285 | <0.001 | | | |
| 0-1+ | 101(41.1) | 24(82.8) | | | | | Ref. |
| 2+ | 58(23.6) | 4(13.8) | | | 0.375 | 0.118-1.198 | 0.098 |
| 3+ | 87(35.4) | 1(3.4) | | | 0.100 | 0.012-0.843 | 0.034 |
| Ki67 | | | 17.151 | <0.001 | | | |
| Low | 96(39.0) | 23(79.3) | | | | | Ref. |
| High | 150(61.0) | 6(20.7) | | | 0.297 | 0.102-0.867 | 0.026 |

作者贡献声明:

王水设计本研究的方案,对稿件的重要内容进行了修改;瞿颖起草和撰写文稿,获取、分析、解释本研究的数据;黄越、李明卉和孙畅对分析解释本研究的数据,对稿件内容进行了修改。

Author's Contributions:

WANG Shui designed the research and made significant revisions to the manuscript; QU Ying drafted and wrote the manuscript, obtained, analyzed, and interpreted the data of this study; HUANG Yue, LI Minghui, and SUN Chang analyzed and interpreted the data of this study and revised the content of the manuscript.

[参考文献]

[1] BRAY F, LAVERSANNE M, SUNG H Y A, et al. Global cancer statistics 2022: GLOBOCAN estimates of incidence and mortality worldwide for 36 cancers in 185 countries[J]. CA-Cancer J Clin, 2024, 74(3): 229-263

[2] FISHER B, REDMOND C, POISSON R, et al. Eight-year results of a randomized clinical trial comparing total mastectomy and lumpectomy with or without irradiation in the treatment of breast cancer[J]. N Engl J Med, 1989, 320(13): 822-828

[3] VERONESI U, CASCINELLI N, MARIANI L, et al. Twenty-year follow-up of a randomized study comparing breast-conserving surgery with radical mastectomy for early breast cancer[J]. N Engl J Med, 2002, 347(16): 1227-1232

[4] DUFFY S W, VULKAN D, CUCKLE H, et al. Effect of mammographic screening from age 40 years on breast cancer mortality(UK age trial): final results of a randomised,

controlled trial[J]. Lancet Oncol, 2020, 21(9): 1165-1172

[5] SAZ-PARKINSON Z, DUFFY S W, CANELO-AYBAR C, et al. Breast cancer screening and diagnosis[J]. Ann Intern Med, 2020, 172(12): 840-841

[6] STEINHOF-RADWANSKA K, LOREK A, HOLECKI M, et al. Multifocality and multicentricity in breast cancer: comparison of the efficiency of mammography, contrast-enhanced spectral mammography, and magnetic resonance imaging in a group of patients with primarily operable breast cancer[J]. Curr Oncol, 2021, 28(5): 4016-4030

[7] GREENWOOD H I, WILMES L J, KELIL T, et al. Role of breast MRI in the evaluation and detection of DCIS: opportunities and challenges[J]. J Magn Reson Imaging, 2020, 52(3): 697-709

[8] 刘婷婷, 林佳璐, 娄鉴娟, 等. 多参数MRI影像组学评估浸润性乳腺癌HER-2表达状态的临床应用价值[J]. 南京医科大学学报(自然科学版), 2024, 44(2): 218-227

LIU T T, LIN J L, LOU J J, et al. Clinical application value of multi-parameter MRI radiomics evaluation of HER-2 expression status in invasive breast cancer[J]. Journal of Nanjing Medical University(Natural Sciences), 2024, 44(2): 218-227

[9] WEAVER O, YANG W. Imaging of breast cancers with predilection for nonmass pattern of growth: invasive lobular carcinoma and DCIS-Does imaging capture it all?[J]. AJR Am J Roentgenol, 2020, 215(6): 1504-1511

[10] ROQUE R, CORDEIRO M R, ARMAS M, et al. The accuracy of magnetic resonance imaging in predicting the size of pure ductal carcinoma in situ: a systematic review and

- meta-analysis[J]. NPJ Breast Cancer, 2022, 8(1): 77
- [11] LEE J, JUNG J H, KIM W W, et al. Efficacy of breast MRI for surgical decision in patients with breast cancer: ductal carcinoma in situ versus invasive ductal carcinoma [J]. BMC Cancer, 2020, 20(1): 934
- [12] AVDAN ASLAN A, GÜLTEKIN S, ESENDAĞLI YILMAZ G, et al. Is there any association between mammographic features of microcalcifications and breast cancer subtypes in ductal carcinoma in situ? [J]. Acad Radiol, 2021, 28(7): 963-968
- [13] KIM J H, KO E S, KIM D Y, et al. Noncalcified ductal carcinoma in situ: imaging and histologic findings in 36 tumors [J]. J Ultrasound Med, 2009, 28(7): 903-910
- [14] JI Y, LI B X, ZHAO R, et al. The relationship between breast density, age, and mammographic lesion type among Chinese breast cancer patients from a large clinical dataset [J]. BMC Medical Imaging, 2021, 21(1): 30-39
- [15] BAE J M, SHIN S Y, KIM E H, et al. Distribution of dense breasts using screening mammography in Korean women: a retrospective observational study [J]. Epidemiol Health, 2014, 36(3): e2014027
- [16] KORHONEN K E, ZUCKERMAN S P, WEINSTEIN S P, et al. Breast MRI: false-negative results and missed opportunities [J]. Radiographics, 2021, 41(3): 645-664
- [17] SHIRAISHI M, IGARASHI T, TERAYAMA T, et al. Breast magnetic resonance imaging for estimation of the tumour extent in patients with pure ductal carcinoma in situ: comparison between full diagnostic and abbreviated protocols [J]. Eur J Radiol, 2020, 123(2): 108788
- [18] LUO H, ZHAO S, YANG W, et al. Preoperative prediction of extensive intraductal component in invasive breast cancer based on intra- and peri-tumoral heterogeneity in high-resolution ultrafast DCE-MRI [J]. Sci Rep, 2024, 14(1): 17396
- [19] LAM D L, SMITH J, PARTRIDGE S C, et al. The impact of preoperative breast MRI on surgical management of women with newly diagnosed ductal carcinoma *in situ* [J]. Acad Radiol, 2020, 27(4): 478-486
- [20] COZZI A, DI LEO G, HOUSSAMI N, et al. Preoperative breast MRI positively impacts surgical outcomes of needle biopsy-diagnosed pure DCIS: a patient-matched analysis from the MIPA study [J]. Eur Radiol, 2024, 34(6): 3970-3980
- [21] TAYLOR D B, BURROWS S, DESSAUVAGIE B F, et al. Accuracy and precision of contrast enhanced mammography versus MRI for predicting breast cancer size: how "good" are they really? [J]. Br J Radiol, 2023, 96(1144): 20211172
- [收稿日期] 2025-02-27
(本文编辑:唐震)

(上接第765页)

- sis of bipolar disorder [J]. Front Psychiatry, 2020, 11: 500
- [46] 任志斌, 金卫东, 王鹤秋. 单相与双相抑郁患者事件相关电位 P50 和 P300 比较 [J]. 临床精神医学杂志, 2016, 26(5): 326-328
- REN Z B, JIN W D, WANG H Q. Comparison of event-related potentials P50 and P300 in patients with unipolar and bipolar depression [J]. Journal of Clinical Psychiatry, 2016, 26(5): 326-328
- [47] KIM Y R, PARK Y M. Mismatch negativity and loudness dependence of auditory evoked potentials among patients with major depressive disorder, bipolar II disorder, and bipolar I disorder [J]. Brain Sci, 2020, 10(11): 789
- [48] BARREIROS A R, BREUKELAAR I A, CHEN W T, et al. Neurophysiological markers of attention distinguish bipolar disorder and unipolar depression [J]. J Affect Disord, 2020, 274: 411-419
- [49] DONALDSON K R, NOVAK K D, DAN F T, et al. Associations of mismatch negativity with psychotic symptoms and functioning transdiagnostically across psychotic disorders [J]. J Abnorm Psychol, 2020, 129(6): 570-580
- [50] 沈梦婷, 张选红, 钱祺颖, 等. 精神分裂症与抑郁症失匹配负波异常的对照研究 [J]. 上海交通大学学报(医学版), 2021, 41(8): 1041-1045
- SHEN M T, ZHANG X H, QIAN Z Y, et al. Comparative study of mismatch negativity abnormalities in schizophrenia and depression [J]. Journal of Shanghai Jiaotong University (Medical Science), 2021, 41(8): 1041-1045
- [51] ZHOU X B, LIN Z H, YANG W Q, et al. The differences of event-related potential components in patients with comorbid depression and anxiety, depression, or anxiety alone [J]. J Affect Disord, 2023, 340: 516-522
- [52] DAYAN-RIVA A, BERGER A, ANHOLT G E. Affordances, response conflict, and enhanced-action tendencies in obsessive-compulsive disorder: an ERP study [J]. Psychol Med, 2021, 51(6): 948-963
- [收稿日期] 2025-01-19
(本文编辑:蒋莉)